

Ground state study of simple atoms within a nano-scale box

M. Neek-Amal^{1,2}, G. Tayebirad³, M. Molayem³,
M. E. Foulaadvand^{1,3}, L. Esmaeili-Sereshki⁵ and A. Namiranian^{1,3}

¹*Department of Nano-Science, Institute for Studies in Theoretical Physics
and Mathematics (IPM), P.O. Box 19395- 5531, Iran.*

²*Department of Physics, Shahid Rajaei University, Lavizan, Tehran 16788, Iran.*

³*Department of Physics, Iran University of Science and Technology, P.O. Box 16844, Iran.*

⁴*Department of Physics, Zanzan University, P.O. Box 45195-313, Zanzan, Iran.*

⁵*Department of Physics, Alzahra University, P.O. Box 15815-3487, Tehran, Iran.*

Ground state energies for confined hydrogen (H) and helium (He) atoms, inside a penetrable/impenetrable compartment have been calculated using Diffusion Monte Carlo (DMC) method. Specifically, we have investigated spherical and ellipsoidal encompassing compartments of a few nanometer size. The potential is held fixed at a constant value on the surface of the compartment and beyond. The dependence of ground state energy on the geometrical characteristics of the compartment as well as the potential value on its surface has been thoroughly explored. In addition, we have investigated the cases where the nucleus location is off the geometrical centre of the compartment.

PACS: 02.70.Ss, 02.70.Uu

Keywords: Ground state energy, Diffusion Monte Carlo, Off centre effects, Confined atoms.

I. INTRODUCTION

In the past few years, spatially confined atoms and molecules have gained relentless attention [1]. This comes mainly from the notable difference between the ground state properties of such confined systems in comparison to their bulk states. As a result, the confining systems may be applied in several circumstances. At present, it is argued that physics of high pressure materials can be investigated within models of confining particles. Furthermore, extensive investigations over large classes of nano-structure systems such as quantum dots and artificial atoms are essentially related to the problem of confined atoms and electrons [2]. By the issue *confined atoms*, we mean the atoms that experience external potentials which keep themselves in a region with length scales comparable to the atomic size. Certainly the boundaries of such regions are not fully impenetrable, and particles are then able to escape from the region. Generally the confining surface is not spherical. The energy spectrum of H and He-atom in penetrable/impenetrable spherical and ellipsoidal boxes have been studied by several authors who have employed several approaches [3, 4, 5, 6, 7, 8, 9]. In all of these models, it is assumed that confining potential only acts up to a cut-off boundary, and do not disturb the atomic Hamiltonian inside the region. Under this simplification, the problem of confined atoms, would be equivalent to the problem of many-body Schrödinger equation with a given boundary condition. Practically, finding the solution of many-body Schrödinger equation with specified boundary condition, is not an easy task even by numerics. As a simple but less accurate method to solve this equation, self consistent Hartree-Fock, or variational techniques are usually taken into account. Another methodology for solving many-body problems,

is Quantum Monte Carlo (QMC) method. This method is among the most powerful methods in obtaining the ground state energy of a many-body system, such as two-electron atoms constrained in spherical impenetrable boxes [10]. In this article, we have used a familiar variant of QMC technique the so-called *diffusion* QMC method [11, 12] to obtain the ground state energy of the simplest confined atoms i.e.; H and He. Our motivation arises from the fact that in real confined atoms, the location of the nucleus does not exactly coincides with the centre of boxes. Since the analytical approaches fail in these cases, employing numerical techniques is inevitable. In order to take into account the effects of size, shape and the potential of the boundary on the ground state energy of confined H and He atoms, we have examined two geometries namely spherical, and ellipsoidal compartments with different sizes and potentials at their boundaries. It is worthwhile to note that the problem of H-atom inside a sphere or cylinder, as a model for H absorption in fullerene or carbon nanotube [15, 16, 17], has found applications in the condensed matter physics. Moreover, the problem of confining He, as the simplest problem combining repulsive electron-electron interaction effect with the repulsion resulting from confinement, could be of interest from theoretical point of view. For example in the finite temperature we expect an ellipsoidal shape for C₆₀ molecule instead of a spherical geometry and in this case one can model this molecule by a prolat-shaped cage [14].

Our new findings can be summarized as follows. We have proposed a set of trial wave functions for H-atom and He-atom in a penetrable/impenetrable spherical and ellipsoidal box and computed the effect of off centrality on the ground state energy for various radii and penetrability. We recall that for these types of atoms, the number of electrons are less than three. Under this con-

dition, it would not be vital to use the fixed node approximation as is used for fermionic systems [13]. We first try to solve the centrally symmetric problems, and then will consider generalizations which involve the effect of displacing the nucleus off the geometrical centre of the compartments. The paper has the following organization: In sec. II we briefly describe our used model. Sec. III reviews the basic ingredients of DMC method and the specific algorithm used in the paper. In Sec. IV we have introduced the used trial wavefunctions and sec. V includes the main results. The paper is ended in sec. VI by some concluding remarks and discussions.

II. THE MODEL

Consider a simple atom subjected to a constant external potential V_0 which acts beyond the exterior region of an encompassing compartment. The time-independent Schrödinger equation for such H-atom is:

$$H\psi(\mathbf{R}) = E\psi(\mathbf{R}). \quad (1)$$

where

$$H(\mathbf{R}) = T(\mathbf{R}) + V_{en}(\mathbf{R}) + V_{ee}(\mathbf{R}) + V_{ext}(\mathbf{R}), \quad (2)$$

here $\mathbf{R} = (\mathbf{r}, \mathbf{x})$ and \mathbf{r}, \mathbf{x} denote the coordinates of the electrons and the nucleus respectively. T is the kinetic energy term for electrons. The nucleus is assumed immobile due to its large mass compared to electron's mass. V_{en} is the Coulombic interaction potential between the electrons and the nucleus and V_{ext} is the external applied potential. V_{ee} is the electron-electron interaction for many electron systems which is zero beyond boundaries. The external potential is zero inside the compartment and constant V_0 on its surface and beyond.

III. DIFFUSION MONTE CARLO METHOD FOR SOLVING SCHRÖDINGER EQUATION

In this section we briefly outline the main ingredients of the Diffusion Monte Carlo scheme. The essence of DMC lies in mapping the Schrödinger equation in imaginary time onto a diffusion-like equation [11, 18]. Through an analytic continuation of time $t \rightarrow -i\tau$ to imaginary values, the Schrödinger equation will appear in the following form:

$$\hbar \frac{\partial \psi(\mathbf{R}, \tau)}{\partial \tau} = D \nabla_{\mathbf{r}}^2 \psi(\mathbf{R}, \tau) - V(\mathbf{R}) \psi(\mathbf{R}, \tau). \quad (3)$$

In which the constant D is $\frac{\hbar}{2m}$. This equation describes the diffusion of an ensemble of interacting particles subject to death and/or growth processes depending on the sign of $V(\mathbf{R})$. The rate of death or growth i.e.; $-V(\mathbf{R})$ is not constant but rather space-dependent. In the long time limit, $\psi(\mathbf{R}, \tau)$ tends to a unique value

$\psi_s(\mathbf{R})$ which is a functional of the potential $V(\mathbf{R})$ which is identical to the ground state wave function of the original quantum mechanical problem. In many situations, $\psi(\mathbf{R})$ shows divergent to infinity or convergent to zero types of behaviour. For examples if $-V(\mathbf{R})$ is positive, as in the hydrogen atom with potential $V(r) = \frac{-e^2}{r}$, Evidently $\psi_s(x)$ diverges because after a sufficient time, the number of particle in the ensemble diverge due to creation process. Now to remedy the problem, one adds a trial constant E_T into the imaginary time Schrödinger equation as follows:

$$\hbar \frac{\partial \psi(\mathbf{R}, \tau)}{\partial \tau} = D \nabla_{\mathbf{r}}^2 \psi(\mathbf{R}, \tau) + (E_T - V(\mathbf{R})) \psi(\mathbf{R}, \tau). \quad (4)$$

In the limit $\tau \rightarrow \infty$, $\psi(\mathbf{R}, \tau)$ will only tends to a non zero and finite value provided E_T coincides with the system ground state E_0 . To make this approach applicable, we can exploit different methods of solving diffusion-like equation such as random walk and Green function. Although a significant advantage of the diffusion Monte Carlo is that one does not need to specify a trial wave function, to speed up the implementation of the method and to avoid errors arising in the problems containing singularities in the potential, it would be helpful to use a guiding trial wavefunction. More specifically, in the positions of singularities, where $V(\mathbf{R})$ diverges, the creation/annihilation rate $E_T - V(\mathbf{R})$ becomes tremendously large and can cause undesirable fluctuation in the number of diffusive particles which makes the algorithm unstable. To smooth this singularities, one uses a time independent trial wavefunction $\psi_T(\mathbf{R})$. To implement this idea, we introduce a function $\rho(\mathbf{R}, \tau)$ defined as $\rho(\mathbf{R}, \tau) = \psi_T(\mathbf{R}) \psi(\mathbf{R}, \tau)$. Substituting $\psi(\mathbf{R}, \tau)$ in terms of ρ in equation (4) gives the following equation:

$$\begin{aligned} \hbar \frac{\partial \rho(\mathbf{R}, \tau)}{\partial \tau} &= D \nabla_{\mathbf{r}} [\nabla_{\mathbf{r}} - F(\mathbf{R})] \rho(\mathbf{R}, \tau) \\ &- (E_L(\mathbf{R}) - E_T) \rho(\mathbf{R}, \tau). \end{aligned} \quad (5)$$

The term $F(\mathbf{R}) = \frac{2 \nabla \psi_T(\mathbf{R})}{\psi_T(\mathbf{R})}$ is called *Fokker-Planck* force and corresponds to force function which drifts the walkers away from regions where $|\psi_T(\mathbf{R})|^2$ is small. The local energy function $E_L(\mathbf{R})$ is defined as $\frac{-D \nabla_{\mathbf{r}}^2 \psi_T(\mathbf{R})}{\psi_T(\mathbf{R})} + V(\mathbf{R})$. An appropriate choice of the trial wavefunction $\psi_T(\mathbf{R})$ gives rise to non singular $E_L(\mathbf{R})$. The method we have taken into account is based on the Green's function approach to equation (5). We recall that the Green's function of equation (5) can not be obtained exactly. However, the problem can be treated using an approximate Green's function for short time evolution. The appropriate approximated Green's function is divided into two terms [18] which are given below:

$$G_D(\mathbf{R}, \mathbf{R}', \Delta\tau) = \frac{\exp(-\frac{(\mathbf{R}' - \mathbf{R} - D\mathbf{F}(\mathbf{R})\Delta\tau)^2}{4D\Delta\tau})}{(4\pi D\Delta\tau)^{3N/2}} + O(\Delta\tau)^2, \quad (6)$$

for diffusive term and

$$G_B(\mathbf{R}', \mathbf{R}, \Delta\tau) = \exp[-\Delta\tau(\frac{E_L(\mathbf{R}) + E_L(\mathbf{R}')}{2} - E_T)], \quad (7)$$

for the branching term. This is the part of the Green's function responsible for the stochastic creation/annihilation process. To improve the error of the order $(\Delta\tau)^2$, we have used the Metropolis procedure which will be explained shortly. Throughout the paper, we have used the following atomic units $\hbar = m = e = 1$. We note that the atomic unit of length is the Bohr radius $\frac{\hbar^2}{me^2} = 0.529 \text{ \AA}$; the time unit is $\frac{\hbar^3}{me^4} = 2.419 \times 10^{-22} \text{ fs}$ and the energy unit is *Hartree* i.e.; $\frac{me^4}{\hbar^2} = 27.25 \text{ eV}$.

A. DMC steps

In what follows we give the algorithmic steps for implementation of the method described above. Firstly, we initialize the system. A number N_0 of non interacting particles (random walkers) are distributed in space. It is preferable to distribute them according to an approximate guess of the ground state wavefunction. Then the position and number of walkers are updated according to the following stochastic rules. These rules are applied synchronously to all the walkers of the ensemble. During an MC step, each walker execute a guided discrete time random walk. To this end, we choose a constant time interval $\Delta\tau$ between walks. The walk length and its direction are stochastic variables. Since the walk is directed, it contains a directed plus a random component. More precisely, the new position of each particle is update according to the following rule:

$$\mathbf{R}' = \mathbf{R} + D\Delta\tau\mathbf{F}(\mathbf{R}) + \eta\sqrt{\Delta\tau}, \quad (8)$$

In which η is a Gaussian random number with zero mean and unit variance. The term $D\Delta\tau\mathbf{F}(\mathbf{R})$ corresponds to the guided part. The attempted move is accepted if the Metropolis test is successful. This test introduces a ratio w given as below:

$$w = \frac{G(\mathbf{R}, \mathbf{R}', \Delta\tau)\rho(\mathbf{R}')}{G(\mathbf{R}', \mathbf{R}, \Delta\tau)\rho(\mathbf{R})} \simeq \frac{G(\mathbf{R}, \mathbf{R}', \Delta\tau)\psi_T^2(\mathbf{R}')}{G(\mathbf{R}', \mathbf{R}, \Delta\tau)\psi_T^2(\mathbf{R})}. \quad (9)$$

The move is accepted with the probability w . The next stage simulates creation/annihilation processes. After accepting the move, we evaluate the branching factor $q = e^{-\Delta\tau(\frac{E_L(\mathbf{R}) + E_L(\mathbf{R}')}{2} - E_T)}$. Let $[q]$ denote the integer part of q and $q - [q]$ its fractional part. When q is greater than one, with the probability $q - [q]$, $[q] + 1$ replicas

and with the probability $1 - (q - [q])$, $[q]$ replicas are replaced at the updated location of the particle to the ensemble of particles. Note that if q is less than one, with probability $1 - q$ the particle annihilates. After performing the above diffusion/branching processes for all the particles in the ensemble, and hence updating the ensemble number N , the final MC step consists of updating the value of E_T . Among various choices of updating rule, we have chosen the following one:

$$E_T = \langle E_L \rangle - \frac{N - N_0}{N_0 \Delta\tau} \quad (10)$$

Where N_0 refer to the initial number of walkers, N denotes the updated number of walkers. The average is an ensemble average. This adjusting of E_T is essential to avoid large fluctuation in the walkers number. After a sufficient MC steps, the time series E_T reaches a steady state. The ground state of the system is obtained by averaging E_T over many MC steps.

IV. TRIAL WAVEFUNCTIONS

A. Spherical penetrable boundaries: Centered atom

In this paper, we have used trial wavefunctions which are appropriately chosen associated to the spherical boundary condition. We note that the potential takes a constant value V_0 on the boundary and beyond it. For the spherical boundary a denotes the radius of the sphere. The impenetrable case has already been done in [10].

When the boundaries are penetrable, for H-atom, we have used an iterative scheme to find the appropriate trial wavefunction. This scheme is implemented according to the following steps: at first we employ the same unbiased method used in [11], for producing the radial wavefunction for all values of V_0 and a . After obtaining the required data for the radial wavefunction, in the second step we find the best fit of the following function to these data. We propose the trial wave function as follows:

$$\Psi_T^H(r, V_0) = Y_3 \exp(-Y_1 r^3 - Y_2 r^2 - Y_0 r). \quad (11)$$

The fitted function $\Psi_T^H(r)$ is in turn used as the trial wavefunction. We note the parameters Y_i 's are functions of V_0 and a . By using the cusp condition, $\psi_T'(r) + \psi_T(r) = 0$, we can determine one of the above parameters such as Y_0 which is equal to one. This condition guarantees singularity cancelation at regions where r is small. The values of the fitting parameters are exhibited for some values of a and V_0 in Table I. In this case E_L for $r < a$ turns out to be

$$E_{LH}(r, V_0) = \frac{1}{2} \left[(6Y_1 r + 2Y_2) - (3Y_1 r^2 + 2Y_2 r + Y_0)^2 \right] - \frac{1}{r} [-3Y_1 r^2 - 2Y_2 r - Y_0 + 1]$$

For exterior regions where $r > a$ the local energy should change to $E_{LH}(r, V_0) + \frac{1}{r} + V_0$. Note that the local energy is obviously finite in the region $r > a$. In the case of He atom inside a penetrable sphere the trial wave function is $\Psi_T^H(\mathbf{r}_1)\Psi_T^H(\mathbf{r}_2)J(r_{12})$. Here the Jastrow function has the form $J(r_{12}) = e^{\frac{r_{12}}{2(1+\alpha r_{12})}}$ with r_{12} as the distance between two electrons and $\alpha = 0.2$. The cusp condition leads us to choose $Y_0 = 2$. Then the local energy when $r_1 < a$ and $r_2 < a$ is written as below

$$E_{LHe}(r, V_0) = E_{LH}(r_1, V_0) + E_{LH}(r_2, V_0) + \frac{1}{r_{12}} - \sum_{i=1}^2 \left[\frac{\nabla_i \Psi_i}{\Psi_i} \cdot \frac{\nabla_i J}{J} + \frac{1}{2} \frac{\nabla_i^2 J}{J} \right]$$

where as before $J = J(r_{12})$ and $\Psi_i = \Psi_T^H(r_i, V_0)$ according to equation (11). In the case of $r_1 > a$ or $r_2 > a$ when one electron goes outside of the sphere the local energy is written as

$$E_{LHe}(r, V_0) + \left[\frac{1}{r_k} - \frac{1}{r_{12}} + V_0 \right]$$

In the above equation k refers to the index of electron in outside region. Finally when both electrons are outside the region, i.e., $r_1 > a$ and $r_2 > a$ the local energy should be written as

$$E_{LHe}(r, V_0) + \left[\sum \frac{1}{r_i} - \frac{1}{r_{12}} + V_0 \right].$$

B. Spherical boundaries: Off-centred atom

Now we discuss the off-centrality in the spherical geometries. When the off-centrality is small and the boundaries are impenetrable we have obtained, for H atom, the trial wavefunction by implementing a shift d along the z -direction: $r' = \sqrt{x^2 + y^2 + (z-d)^2} = \sqrt{\rho^2 + (z-d)^2}$.

$$\Psi_{TD}^H(\mathbf{r}') = e^{(-r' + \lambda(z,d)r'^2)} j_0(kr), \quad (12)$$

where $j_0(kr)$ is the zero order Bessel-function with $k = \pi/a$. The first term plays the role of off-centrality and the second term insures the vanishing of the wave function on the borders. Defining $f = e^{-r' + \lambda(z,d)r'^2}$ and using cylindrical coordinates, the local energy is found to have the following form:

$$E_{LD}(\rho, z) = -\frac{1}{2} \left[\frac{d^2 f / d\rho^2}{f} + \frac{1}{\rho} \frac{d \ln f}{d\rho} \right] - \frac{d^2 f / dz^2}{2f} + \frac{k^2}{2} - \hat{r} \left[\hat{\rho} \frac{df}{d\rho} + \hat{z} \frac{df}{dz} \right] \cdot \left[k \cot(kr) - \frac{1}{r} \right] \quad (13)$$

where $\hat{r} = \hat{\rho} + \hat{z}$. For keeping the local energy finite every where especially at $r = a$ one needs to solve an ordinary differential equation for $\lambda(z, d)$. Such solution

is a complex function which in the range $d \leq 0.5a$ has a simple linear behaviour, $\lambda = Az + B$ where A and B depend on d . Table II includes the values of A and B for many geometries.

When the boundaries are penetrable and off-centrality is small, we have used $\Psi_T^H(r', V_0)$ with the same functional form as in the equation (11). The corresponding parameters Y_i 's are taken from Table I.

In the case of small off-centred He atom within an impenetrable spherical box we have used the following trial function:

$$\Psi_{TD}^H(\mathbf{r}'_1)\Psi_{TD}^H(\mathbf{r}'_2)J(r_{12}), \quad (14)$$

where $r'_i = \sqrt{x_i^2 + y_i^2 + (z_i - d)^2}$ and r_{12} is defined as the distance between two electron as before.

C. Ellipsoidal boundaries

In the case of ellipsoidal geometries first we recall the equation of a standard ellipsoid which has been prolated in the z -direction by defining the function $R = \sqrt{\frac{x^2 + y^2}{a^2} + \frac{z^2}{b^2}}$. When $R = 1$ we have an ellipsoid surface with the semi-major axis a and the semi-minor axis b . Without losing generality we assume $b > a$. For small eccentricity i.e., $\epsilon = \sqrt{\frac{b^2}{a^2}} - 1$, our trial wave function for H atom within an impenetrable ellipsoidal boundary is

$$\Psi_{Te}^H(r, R) = e^{(-r + \beta r^2)} j_0(kR). \quad (15)$$

k should be equal to π while $\beta = [2\sqrt{\frac{2a^2 + b^2}{3}}]^{-1}$. These values have been determined by keeping the local energy finite and reaching to the same function of spherical case when $a = b$. For H atom in penetrable boundaries we have used $\Psi_T^H(R, V_0)$ using the functionality analogous to equation (11).

In the case of He atom in a prolated impenetrable ellipsoid with small eccentricity we have used the following wave function $\Psi_{Te}^H(r_1, R_1)\Psi_{Te}^H(r_2, R_2)J(r_{12})$. For He atom in penetrable ellipsoidal boundaries one can replace the first two terms of equation (14) by $\Psi_T^H(R_1, V_0)$ and $\Psi_T^H(R_2, V_0)$ respectively.

V. RESULTS

Prior to presenting our results, it would be illustrative to discuss the numerical errors in the DMC method. Principally, there are two types of errors which limit the accuracy of most DMC calculations: (a) statistical or sampling errors associated with the limited number of independent sample energies used in determining the ground state energy and (b) the systematic errors

associated with finite time-step $\Delta\tau$, round-off in computing, imperfectness of random number generators etc. For a spacial boundary condition like the spherical boxes with penetrable boundaries, we know the energies value (steady state energy) from the analytical calculations ([10]), therefore, minimizing the variance of energy, can give us a range of time step. We have used the minimum of these time step, i.e., $\Delta\tau=0.005$. The number of walkers was taken $N_0 = 5000$ in our simulation.

A. Spherical box

The first quantity that we have calculated is the electronic ground state wavefunction (see Fig. 1). Due to spherical symmetry, the solution of the Schrödinger equation can be solved by separating the variables so that the wavefunction is represented by the product $\psi(r, \theta, \phi) = \Phi(r)\Theta(\theta)\varphi(\phi)$. Furthermore, because the ground state wavefunction of centred H-atom in a spherical geometry has radial symmetry, one can replace ψ with $r\Phi(r)$ for simplicity. For an atom confined in the centre of an impenetrable and very small sphere ($V_0 = \infty$ and $a=1$), the wavefunction dramatically differs from that of free atom. Accordingly, the maximum of the wavefunction shifts towards smaller r , which also causes larger slope in its curvature (see Fig. 1(a)). On the boundary, the wavefunction tends smoothly to zero. Since kinetic energy corresponds to the Laplacian of the wavefunction, this enhancement of the slope consequently leads to the enhancement of the ground state energy. The situation is significantly different for large encompassing regions where the radius of the sphere is notably greater than one atomic unit. As can be inferred from Fig. 1(b), where $a=4.0$, the electronic wavefunction deviates slightly from the electronic wavefunction of a free H-atom. In this case the wavefunction tends to zero with small slope. Moreover, the influence of V_0 has been suppressed.

An important feature of the electronic wavefunction in small compartments (when $a = 1$) is its dependence on the penetrability V_0 . By decreasing the potential V_0 , the tendency of an electron for being near the boundary increases and for pure penetrable sphere ($V_0 = 0.0$) the probability of finding the electron near the boundary becomes maximum. In Fig. 2(a) we have plotted the ground state energy versus the strength of penetrability for several radii. Apparently, the ground state energy strongly depends on the penetrability when the size of bounded region is comparable to the volume of a free H-atom, i.e., $a \leq 1$. Nonetheless, for larger regions and larger radii, ground state energy is almost independent of V_0 .

To improve our understanding, in the set of coloured two dimensional figures, we have depicted the behaviour of electronic distribution (see Fig. 3-5) for some values of V_0 at $a = 1$ in the $x-z$ plane. As can be seen, by increasing V_0 , the electronic distribution becomes more localized around the nucleus and keeps its symmetry independent

of V_0 . In the case of fully penetrable boundary, electron has access to exterior regions. The blue regions represent a smaller probability for finding the electron, whereas the red regions represent higher probabilities. The electron does not penetrate to the exterior regions in deeper confining potential barrier.

B. Off-centred atoms

One of the most significant advantages of DMC method lies in its simplicity in being applied to various boundary conditions. This property allows us to investigate the effect of displacement of H-atom along the z -direction on the ground state energy of the system. Our motivation in considering this geometrical case is two-fold: first, in real systems (such as confined atoms in a metallic bubble) one can not fix the atoms on the geometrical centre and second, due to mathematical difficulties arising from the analytical treatments. Figure 2(b) illustrates the results of this investigation for three values of V_0 . The figure depicts the ground state energy of a H-atom confined in a sphere with radius $a = 1$ versus the nucleus displacement d (in atomic unit) from centre of the sphere. Generically, the off-centre effects become more considerable when the displacement d exceeds nearly half of the radius a . Table III contains our results for ground state energy. Our energy results for the case $d = 0$ and impenetrable boundaries are in good agreement with those in [10]. For the case of penetrable boundaries our results are in well agreement with the analytical results in [5]. For a deeper understanding, we exhibited the dependence of the energy on the displacement d in Fig. 2(c) for impenetrable sphere. For larger a the deviation of the energy occurs in larger displacement d .

For off centred helium atom all the results are shown in table IV. The general behaviour is qualitatively analogous to the H- atom. However, due to electron-electron interaction, geometrical effects are suppressed compared to H- atom case. Our results for $d = 0$ and impenetrable boundaries are in reasonable agreement with the results given in [10]. It has been verified that if one uses a local and negative penetrability in the boundaries when the atom moves towards the boarder, the electron can cross the well depending on the well deep [16].

C. Ellipsoidal box

Let us now investigate the ground state energy of a H- and a He- atom confined within an ellipsoidal compartment. We consider a symmetric type of ellipsoid characterized by parameters a and b which are semi-major and semi-minor axes respectively. For simplicity, we have used small eccentricity, i.e, $b = 1.1a$ and $b = 1.5a$ for several a and V_0 . We recall that nucleus is placed in the centre.

The ground state energy of H-atom confined in larger ellipsoidal cavity (large a and b) tends to the energy of the ground state of free H-atom, -0.5 , see table V. When we increase V_0 to a higher value we observe that energy increases especially for smaller a . For a fixed a , larger b has larger energy in all cases. For an ellipsoid with small semi-major axis, the ground state energy will be more affected by the surrounding potential.

For many-particle systems, finding an exact solution of the Schrödinger equation is merely possible and approximate methods should inevitably be taken into account. The ground state wavefunction of He-atom is node-less and the Pauli exclusion principle does not play a significant role. For this reason the above simple DMC method is reasonable. In table VI we have reported energy values of He-atom in several ellipsoidal geometries. All used parameters such as a , b are defined similar to the H-atom case. By increasing a and b the ground state energy asymptotically tends to the lowest state energy of free He-atom i.e. -2.903 au. In small radius the energies have larger values, because electrons are closer to each other and to the nucleus. For higher values of V_0 , two electrons are confined only inside the box and interact via Coulombic forces, therefore the energy should be increased. The elimination of the electron-electron interaction decreases the ground state energy in comparison to the case where this interaction is on.

In the absence of nucleus, systems with the larger val-

ues of a and b behave as a 2-dimensional confined electron gas which are vastly studied in quantum dots [19].

VI. SUMMARY

In this paper we have evaluated the ground state energies and wavefunctions of confined Hydrogen and Helium atoms by the method of Diffusion Monte Carlo. In particular, we have studied spherical and ellipsoidal confining compartments. Ground state values crucially depend on the size of confining compartments. In larger compartments, the results asymptotically approach to the values of free atoms. The effect of displacing the nucleus from the geometrical centre of the confining region has also been investigated. This effect is of theoretical as well as practical interest. We have shown that the ground state energies for both H and He atoms inside the ellipsoidal box significantly depend on the position of nucleus and the penetrability of boundaries. The merit of DMC is that it simply can treat an arbitrary shape of boundaries. Our future work will be devoted to find a reasonable model for confined atoms within a carbon nano-tube and correspondingly applying QMC methods on such a systems with a cylindrical confinement. Work along this line is in progress and will be reported elsewhere.

-
- [1] W. Jaskolski, Phys. Rep. 271, 1 (1996).
 - [2] T. Sako and G. H. F. Diercksen, J. Phys. B At. Mol. Opt. Phys. 36, 1433 (2003).
 - [3] E. V. Ludena, J. Chem. Phys. 69, 1170 (1978).
 - [4] E. V. Ludena and M. Gregori, J. Chem. Phys. 71, 2235 (1979).
 - [5] E. Ley-Koo and S. Rubinstein, J. Chem. Phys., 71, 351 (1979).
 - [6] S. H. Patil, J. Phys. B: At. Mol. Opt. Phys., 34 1049 (2001).
 - [7] N. Aquino, A. F-Riveros and J. F. Rivas-Silva, Phys. Lett. A. 307, 326 (2003), N. Aquino, J. Garza, A. Flores-Riveros, J. F. Rivas-Silva and K. D. Sen, J. Chem. Phys., 124, 054311 (2006).
 - [8] C. Laughlin, B. L. Burrows and M. Cohen, J. Phys. B: At. Mol. Opt. Phys. 35, 701 (2002).
 - [9] D. Djajaputra and B. R. Cooper, Eur. J. Phys. 21, 261 (2000).
 - [10] C. Joslin and S. Goldman, J. Phys. B: At. Mol. Opt. Phys. 25, 1965 (1992).
 - [11] I. Kosztin, B. Faber and K. Schulten, Am. J. Phys. 64, 633 (1996).
 - [12] P. R. Charles Kent, 1999, Ph.D. thesis, University of Cambridge.
 - [13] P. J. Reynolds, D. M. Ceperley, B. J. Alder and W. A. Lester Jr, J. Chem. Phys., 77, 5593 (1982).
 - [14] J. P. Connerade, A. G. Lyalin, R. Semaoune, S. K. Semenov and A. V. Solov'yov, J. Phys. B: At. Mol. Opt. Phys. 34 (2001) 2505-2511.
 - [15] W. Liang, M. Bockrath and H. Park, Phys. Rev. Lett. 88, 126801 (2002).
 - [16] M. Neek-Amal, G. Tayebirad and R. Asgari, J. Phys. B: At. Mol. Opt. Phys. 40 (2007) 1509-1521.
 - [17] K. D. Sen, J. Chem. Phys. 122 (2005) 194324
 - [18] W. M. C. Foulkes, L. Mitas, R. J. Needs and G. Rajagopal, Rev. Mod. Phys. 73, 33 (2001).
 - [19] G. Cantele, D. Ninno and G. Iadonisi, J. Phys.: Condens. Matter 12, 9019, (2000).
 - [20] C. Joslin and S. Goldman, J. Phys. B: At. Mol. Opt. Phys. 25 (1992) 1965-1975.

a	V_0	Y_1	Y_2	Y_3	V_0	Y_1	Y_2	Y_3	V_0	Y_1	Y_2	Y_3	V_0	Y_1	Y_2	Y_3	V_0	Y_1	Y_2	Y_3	V_0	Y_1	Y_2	Y_3
1.0		0.0	0.01	2.0		0.0	0.22	3.19		0.08	0.93	4.99		0.01	0.9	4.68		0.06	0.14	3.73		0.02	0.95	4.93
2.0		0.0	0.04	2.23		0.0	0.24	2.89		0.01	0.47	3.41		0.01	0.52	3.35		0.01	0.62	3.31		0.08	0.54	3.39
3.0	0.0	0.0	0.02	2.07	1.0	0.03	0.0	2.14	2.0	0.01	0.3	2.64	3.0	0.01	0.24	2.57	4.0	0.09	0.51	2.89	5.0	0.01	0.83	3.31
4.0		0.0	0.42	2.61		0.01	0.64	2.87		0.01	0.31	2.54		0.01	0.16	2.23		0.03	0.61	2.75		0.02	0.23	2.50
5.0		0.01	0.44	2.59		0.01	0.74	2.90		0.01	0.5	2.66		0.01	0.48	2.51		0.01	0.11	2.24		0.01	0.41	2.61

TABLE I: Values of the fitted parameters needed for trial wavefunctions in spherical penetrable box.

a=1			a=2			a=3			a=4			a=5		
d	A	B	d	A	B	d	A	B	d	A	B	d	A	B
0.1	0.035	0.498	0.2	0.009	0.249	0.3	0.004	0.166	0.4	0.002	0.124	0.5	0.001	0.099
0.2	0.072	0.490	0.4	0.018	0.245	0.6	0.008	0.163	0.8	0.005	0.123	1.0	0.003	0.098
0.3	0.106	0.478	0.6	0.026	0.239	0.9	0.012	0.160	1.2	0.007	0.119	1.5	0.004	0.096
0.4	0.134	0.464	0.8	0.033	0.232	1.2	0.015	0.155	1.6	0.008	0.116	2.0	0.005	0.093
0.5	0.152	0.447	1.0	0.038	0.224	1.5	0.017	0.149	2.0	0.010	0.112	2.5	0.006	0.089

TABLE II: Values of coefficients A and B in sec. IV.B

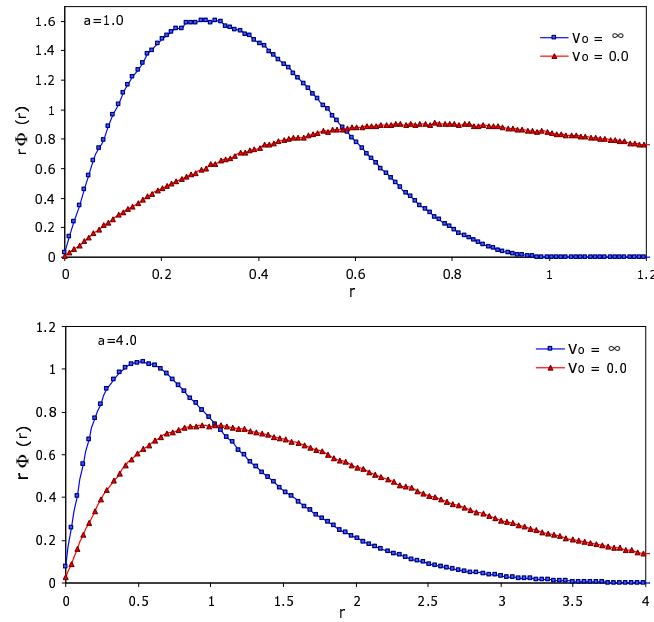


FIG. 1: (Color online) The electronic ground state wavefunction of H-atom confined in a sphere for two values of V_0 . $a = 1$ and 4.0 in (a) and (b) respectively. In both figures $d = 0$.

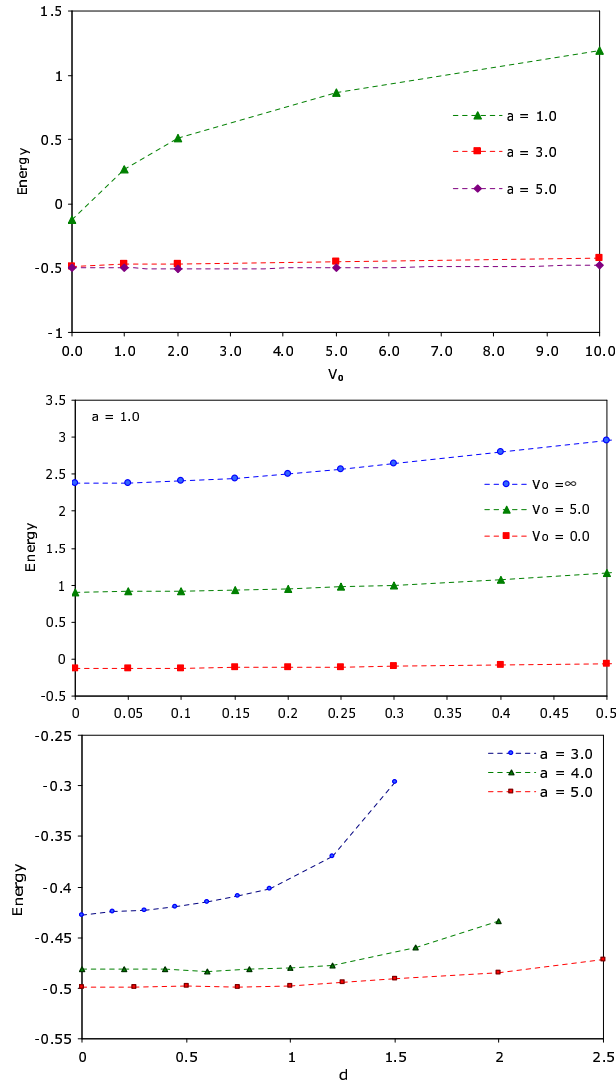


FIG. 2: (Color online) (a) Ground state energy of H-atom versus penetrability in an spherical compartment for various radii when $d = 0$. (b) Ground state energy of confined H-atom for different penetrability coefficients versus off-centre distances d when $a = 1.0$. (c) Ground state energy of a H-atom confined in an impenetrable spherical compartment for various values of a versus off-centre distance d for $V_0 = \infty$.

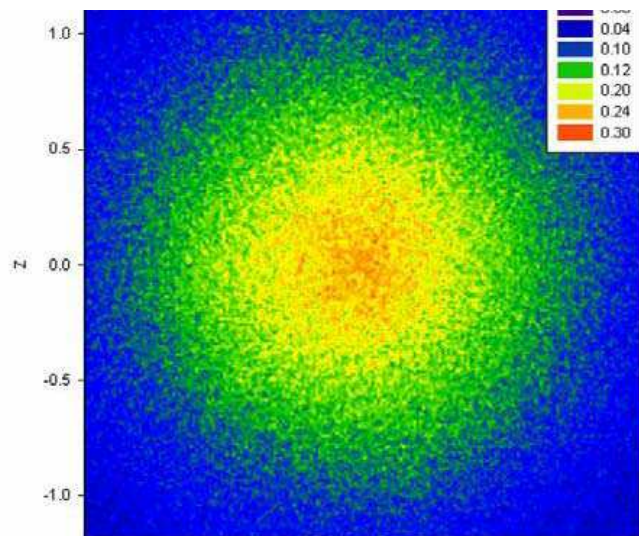


FIG. 3: (Color online) Electronic distribution of H-atom inside a spherical compartment for $V_0 = 0$ and fixed $a = 1$ when $d = 0$.

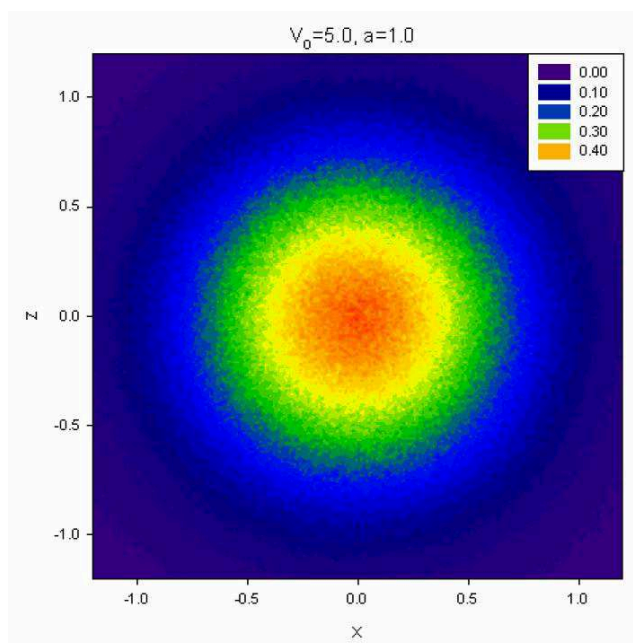


FIG. 4: (Color online) Electronic distribution of H-atom inside a spherical compartment for $V_0 = 5$ and fixed $a = 1$ when $d = 0$.

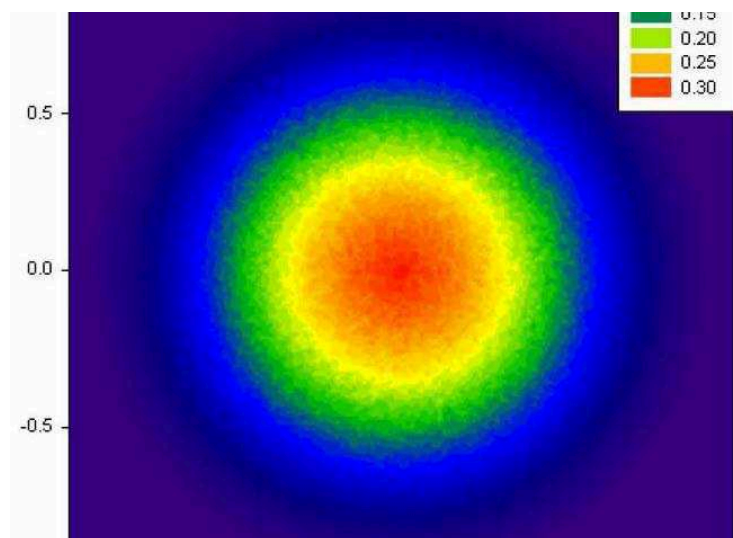


FIG. 5: (Color online) Electronic distribution of H-atom inside a spherical compartment for $V_0 = /infty$ and fixed $a = 1$ when $d = 0$.

a	d	$V_0 = 0.0$	$V_0 = 5.0$	$V_0 = \infty$
1.00	0.00	-0.1250(7)	0.822(7)	2.1760(6)
	0.10	-0.122(8)	0.878(8)	2.5070(7)
	0.20	-0.116(9)	0.918(4)	2.5970(8)
	0.30	-0.102(5)	0.974(6)	2.6210(6)
	0.40	-0.082(9)	1.040(6)	2.711(5)
	0.50	-0.059(7)	1.1450(6)	2.863(1)
2.00	0.00	-0.430(3)	-0.182(1)	-0.1250(6)
	0.20	-0.4280(7)	-0.163(3)	-0.027(8)
	0.40	-0.414(2)	-0.1500(8)	-0.043(7)
	0.60	-0.399(5)	-0.113(6)	-0.0260(3)
	0.80	-0.394(2)	-0.028(1)	0.021(1)
	1.00	-0.383(2)	0.0600(8)	0.110(2)
	3.00	0.00	-0.489(6)	-0.4510(6)
0.30	-0.4840(6)	-0.446(4)	-0.399(8)	
0.60	-0.479(8)	-0.4370(5)	-0.385(6)	
0.90	-0.467(4)	-0.428(4)	-0.384(3)	
1.20	-0.463(8)	-0.404(4)	-0.371(3)	
1.50	-0.4551(4)	-0.351(9)	-0.296(5)	
4.00	0.00	-0.496(3)	-0.489(3)	-0.481(9)
	0.40	-0.493(7)	-0.475(9)	-0.470(3)
	0.80	-0.491(8)	-0.449(1)	-0.465(2)
	1.20	-0.489(9)	-0.470(7)	-0.459(4)
	1.60	-0.480(7)	-0.408(1)	-0.463(5)
	2.00	-0.470(4)	-0.391(4)	-0.435(4)
	5.00	0.00	-0.499(9)	-0.498(6)
0.50	-0.494(7)	-0.490(2)	-0.488(1)	
1.00	-0.485(2)	-0.479(6)	-0.494(7)	
1.50	-0.491(8)	-0.478(8)	-0.486(4)	
2.00	-0.490(6)	-0.469(4)	-0.490(8)	
2.50	-0.499(7)	-0.471(5)	-0.471(6)	

TABLE III: The ground state energy of confined H -atom for various values of penetrability coefficients and off-center distances d .

a	d	$V_0 = 0.0$	$V_0 = 5.0$	$V_0 = \infty$
1.00	0.00	-2.2290(7)	-0.910(5)	1.012(4)
	0.10	-2.228(8)	-0.949(6)	1.105(6)
	0.20	-2.269(2)	-0.965(2)	1.175(9)
	0.30	-2.241(8)	-0.921(4)	1.477(5)
	0.40	-2.250(8)	-0.941(6)	1.926(2)
	0.50	-2.247(4)	-0.916(8)	2.602(7)
2.00	0.00	-2.757(5)	-2.652(6)	-2.603(6)
	0.20	-2.774(7)	-2.619(9)	-2.496(3)
	0.40	-2.747(7)	-2.615(2)	-2.448(7)
	0.60	-2.723(2)	-2.6300(8)	-2.382(6)
	0.80	-2.759(7)	-2.642(8)	-2.247(1)
	1.00	-2.781(3)	-2.622(9)	-2.008(8)
	3.00	0.00	-2.831(4)	-2.776(1)
0.30		-2.797(8)	-2.791(6)	-2.754(6)
0.60		-2.801(1)	-2.805(7)	-2.749(4)
0.90		-2.781(9)	-2.7820(3)	-2.735(4)
1.20		-2.780(2)	-2.757(2)	-2.703(1)
1.50		-2.809(7)	-2.806(6)	-2.607(2)
4.00	0.00	-2.816(5)	-2.803(1)	-2.892(6)
	0.40	-2.771(6)	-2.804(9)	-2.800(1)
	0.80	-2.806(8)	-2.830(1)	-2.795(8)
	1.20	-2.7980(8)	-2.787(4)	-2.781(8)
	1.60	-2.814(1)	-2.792(9)	-2.778(1)
	2.00	-2.801(4)	-2.789(9)	-2.7380(4)
5.00	0.00	-2.812(8)	-2.798(2)	-2.902(7)
	0.50	-2.815(1)	-2.806(1)	-2.8710(8)
	1.00	-2.8280(7)	-2.776(2)	-2.820(9)
	1.50	-2.765(4)	-2.7750(5)	-2.797(5)
	2.00	-2.797(9)	-2.793(7)	-2.812(8)
	2.50	-2.821(6)	-2.791(9)	-2.800(4)

TABLE IV: The ground state energy of confined He -atom for various values of penetrability coefficients and off-centre distances d .

a	b	$V_0 = 0.0$	$V_0 = 5.0$	$V_0 = \infty$	b	$V_0 = 0.0$	$V_0 = 5.0$	$V_0 = \infty$
1.00	1.10	-0.1320(2)	0.819(6)	1.832(1)	1.50	-0.179(2)	0.605(9)	1.460(7)
1.50	1.65	-0.352(1)	-0.013(1)	0.269(8)	2.25	-0.367(9)	-0.095(9)	0.133(8)
2.00	2.20	-0.428(6)	-0.288(8)	-0.184(3)	3.00	-0.443(7)	-0.338(4)	-0.257(8)
2.50	2.75	-0.466(7)	-0.415(1)	-0.374(1)	3.75	-0.476(9)	-0.428(7)	-0.397(2)
3.00	3.30	-0.482(1)	-0.450(5)	-0.434(3)	4.50	-0.485(4)	-0.466(1)	-0.452(2)
3.50	3.85	-0.490(6)	-0.473(4)	-0.477(4)	5.25	-0.489(3)	-0.480(2)	-0.481(2)
4.00	4.40	-0.490(6)	-0.484(5)	-0.492(3)	6.00	-0.492(3)	-0.492(3)	-0.494(6)
4.50	4.95	-0.491(3)	-0.490(6)	-0.489(2)	6.75	-0.497(2)	-0.493(1)	-0.4940(6)
5.00	5.50	-0.490(9)	-0.490(2)	-0.493(7)	7.50	-0.486(5)	-0.497(8)	-0.500(8)

TABLE V: The ground state energy of H-atom confined in an ellipsoidal box, with $b = 1.1a$ and $b = 1.5a$.

a	b	$V_0 = 0.0$	$V_0 = 5.0$	$V_0 = \infty$	b	$V_0 = 0.0$	$V_0 = 5.0$	$V_0 = \infty$
1.00	1.10	-1.6890(3)	-1.101(7)	0.203(4)	1.50	-1.923(3)	-1.429(3)	-0.371(2)
1.50	1.65	-2.544(6)	-2.382(3)	-2.115(6)	2.25	-2.611(9)	-2.502(7)	-2.274(3)
2.00	2.20	-2.795(2)	-2.750(4)	-2.644(3)	3.00	-2.780(6)	-2.772(8)	-2.712(8)
2.50	2.75	-2.881(4)	-2.8350(9)	-2.813(3)	3.75	-2.851(9)	-2.851(6)	-2.820(7)
3.00	3.30	-2.859(7)	-2.874(5)	-2.880(3)	4.50	-2.904(3)	-2.869(3)	-2.8780(6)
3.50	3.85	-2.868(3)	-2.888(7)	-2.908(2)	5.25	-2.885(2)	-2.924(8)	-2.866(8)
4.00	4.40	-2.877(8)	-2.894(4)	-2.865(7)	6.00	-2.8900(6)	-2.881(8)	-2.885(9)
4.50	4.95	-2.8480(1)	-2.895(3)	-2.889(2)	6.75	-2.883(9)	-2.864(9)	-2.860(5)
5.00	5.50	-2.887(2)	-2.9150(8)	-2.899(2)	7.50	-2.889(4)	-2.870(3)	-2.869(3)

TABLE VI: The ground state energy of He-atom confined in an ellipsoidal box, with $b = 1.1a$ and $b = 1.5a$.